Bull. Soc. Photogr. Imag. Japan. (2020) Vol. 30 No. 1: 5–9

Techinical Report

Characterization of Photographic Emulsions for Autoradiography

Ken'ichi Kuge*, Masamichi Okubo**, Naotaka Naganawa***, Hyuma Masu****, Hiroyuki Suzuki*

Abstract: A nuclear emulsion prepared at Nagoya University was verified to be usable for autoradiography in comparison with a commercial emulsion used for this purpose, as production of many silver-salt photographic materials is now discontinued. Photographic characteristics of two nuclear emulsions were estimated in terms of the sensitivity for light and β-rays, and the shapes of silver halide grains and developed silver grains were observed with electron microscopes. Autoradiography with β-rays was conducted by applying the emulsions on a sample with a radioisotope and evaluating the images formed on the emulsions. This emulsion prepared at Nagoya University has properties similar to those of the commercial one and can be used for autoradiography.

Key words: Silver-salt photographic material, nuclear emulsion, discontinuation of commercial production, autoradiography, β-ray

1. Introduction

Autoradiography is a method for analyzing samples using distribution images of the radiation emitted from radioisotopes (RI) contained in the sample[1]. Silver-salt photographic materials or imaging plates are used to detect the radiation from RI. Among these, the former have some advantages, such as providing high-resolution images and the ability to adhere closely to a sample surface of irregular shape.

Because of the recent reduction in the use of silver-salt photographic systems, many photographic emulsions for autoradiography have also been discontinued, and the supply has become dwindling. Under these conditions, Nagoya University launched its own emulsion-production equipment, and emulsions for nuclear plates to detect radiation tracks have been supplied [2].

It may also be possible to apply this emulsion to autoradiography, but no verification has been performed so far. A new type emulsion prepared at Nagoya University [3], which is composed of silver iodo-bromide grains of about 200 nm and has the similar characteristics as those used in the OPERA Experiment for neutrino detection [4,5], is currently used in muon radiography [6,7], gamma-ray telescopes [8] and the search for neutrino [9, 10], among others. We compared the properties of this emulsion with an existing commercially available emulsion for autoradiography to verify whether it can be used for autoradiography.

2. Experimental method

The commercially available emulsion for autoradiography used here was an NTB emulsion made by Eastman Kodak Company (Cat#: 899-5666, hereinafter referred to as Em1). The emulsion made by Nagoya University (referred to as Em2) for track detection described above was used for the comparison. Data, such as the grain size or weight ratio of silver halide to gelatin, has not been obtained for the commercially available Em1. The grain size of Em2 is approximately 220 nm, the standard deviation is 19 nm [11], and the weight ratio of silver halide to gelatin is 3.1:1. The photographic emulsions for track detection, such as Em2, usually maintain similar high ratio to increase the detection efficiency.

Both emulsions were applied to a slide glass and used as dry plates to measure the photographic properties. Em1 was diluted with 1% solution of photographic gelatin to a weight ratio of 1:2, and that for Em2 to 1:3, to lower the viscosity of the emulsion sols for this application. This dilution ratio was increased in Em2 because of the high ratio of silver halide to gelatin (details are described later).

The size and shape of silver halide grains in these emulsions were observed with a transmission electron microscope (TEM; Hitachi, H-7650). The gelatin layer was decomposed with a trypsin solution using a method reported previously [12]. These silver halide grains were subjected to carbon deposition, and the carbon replica after removing the silver halide was observed.

The emulsion layers were observed with a scanning electron microscope (SEM; JEOL, JSM-6510A) at 15.0 kV, and the elemental composition of the layer was measured with an energy dispersive X-ray spectroscopy (EDX) system attached to the microscope. A thin part of the layer surface was removed with a razor to expose the grains buried in the layer, and a layer of gold was sputter-coated on the exposed surface.

Light sensitometry was performed at high-intensity exposure of 10^{-5} s. A sensitometer with a flash lamp as a light source for high-in-

Received 3rd April, 2020; Accepted 30th April, 2020; Published 12th May, 2020.
*Radioisotope Research Center, Chiba University, 1-33 Yayoi-cho, Inage-ku, Chiba 263-8522, Japan
**Department of Anatomy and Neuroscience, Hyogo College of Medicine, 1-1 Mukogawa-cho, Nishinomiya, Hyogo, 663-8501 Japan
***Institute of Materials and Systems for Sustainability, Nagoya University, Furo-cho, Chikusa-ku, Nagoya, 464-8602, Japan
****Center for Analytical Instrumentation, Chiba University, 1-33 Yayoi-cho, Inage-ku, Chiba, 263-8522, Japan.

tensity exposure (EG&G, Mark7) was used. The step exposures through a step wedge were applied to a plate.

β-ray exposure with an average energy of 156 keV emitted from ^{14}C was used to measure radiation sensitivity. The source is a medal-type standard source for calibration of radiation detectors, and the radioactivity was of 3 to 4 kBq. The source was composed of a circle of a polymer layer including ^{14}C approximately 5 mm diameter. We attached photographic plates to several sources one by one consecutively and exposed the β-rays for various exposure times, ranging from 9 h to 18.8 days. After these exposures, we developed the plates simultaneously.

We used D72 developer diluted 5-fold for the development of light sensitometry and sensitivity measurement of β-rays. The development temperature was 20 °C, and the development time was 10 min.

The optical density (OD) of the blackening area after the development process was measured by a densitometer. For the light sensitometry, the OD was measured at four points in the blackening area, corresponding to each stage of the step wedge, and the four OD values were averaged. Because the OD value was not uniform throughout the area of the β-ray exposure, as it was maximized in the center of the area, the OD was measured at several points around the center by shifting the points slightly, and the value showing the maximum was used for the OD by β-ray exposure.

We drew photographic characteristic curves using the light sensitometry, which indicated OD changes to exposure value. The sensitivity for light exposure was measured at the raising point of the characteristic curve and defined as the reciprocal of the exposure value H that gave OD = 0.2 over the fog value. The fog value was determined by the OD in the unexposed area. Gamma was determined by the slope of the straight portion in the characteristic curve. To estimate the β-ray sensitivity, we measured the OD values by the exposure of β-ray from the ^{14}C source of 3 to 4 keV for each exposure time, which gave the OD increasing rate.

The shape of the developed silver particles was observed with the same TEM. We shaved off the emulsion layer at the high-exposure area of the samples used for light sensitometry and decomposed the gelatin with the enzyme solution. A drop of the solution containing dispersed developed-silver particles was placed on a grid covered with a collodion layer and then observed.

Autoradiography was conducted by the method of *in situ* hybridization histochemistry with a labeled compound containing RI of ^{35}S, which is a β-nuclide and emits only β-rays with an average energy of 167 keV [13]. The emulsions were diluted 1:1 with water and were applied to biological sample sections of rat dorsal root ganglion where the labeled compound was distributed. After exposure for 4-8 weeks, these sample sections with the exposed emulsion layer were developed with D19 developer for 3 min at 20 °C. The distribution of developed silver particles on the sample sections was observed with an optical microscope.

3. Experimental results

TEM micrographs of the carbon replica of silver halide grains for Em1 and 2 are shown in Fig. 1. Em1 consists primarily of thick hexagonal flat grains, while spherical and rod-shaped grains are also mixed slightly. The average diameter is 360 nm, but the grain size has a wide size distribution from 100 to 600 nm, and the standard deviation is 130 nm. Em2 consists of monodisperse octahedral grains with diameters of approximately 200 nm, but the edges and corners are rounded, approaching a spherical shape. The average grain size for Em2 was reported to be 220 nm, and the standard deviation was 19 nm [11]. The results obtained here agree with this report.

SEM micrographs of the emulsion layer after shaving off the surface are shown in Fig. 2. The gray areas consisting of circles or hexagons indicate the silver halide grains, and the black area filling in the gap between the grains is the gelatin part as a binder. Highlight areas are the fragments of gelatin fluffing up over the surface after shaving off the surface layer. The shapes of the grains for both emulsions are similar to the results shown in the TEM images in Fig. 1. The grains in Em2 are closely spaced, while the gap between grains is wider in Em1. This indicates that the ratio of gelatin is larger in Em1 than it is in Em2.

The elemental composition measured with EDX in the area observed in SEM is shown in Table 1. Although the silver halide grains in Em2 contain a small amount of iodine, it is expected that the

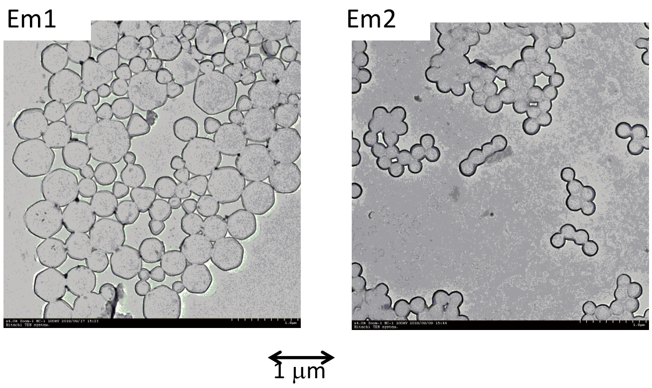

Fig. 1 Transmission electron micrographs of carbon replicas prepared from the emulsion grains for Em1 and 2.

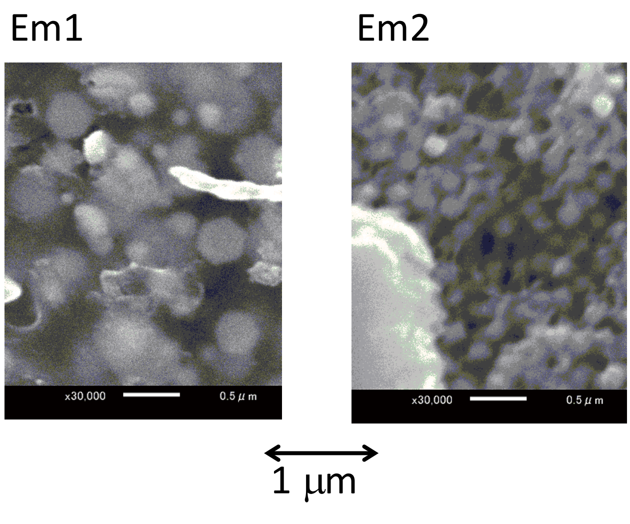

Fig. 2 Scanning electron micrographs of the surface of emulsion layers for Em1 and 2 after shaving off.

atomic ratio of silver to bromine is nearly 1:1. However, the EDX result indicated that this ratio was approximately 1:2, indicating an excess of bromine. One possible explanation is as follows. Because the electron beam was irradiated during the measurement, this beam would decompose some silver bromide to silver atoms and bromine molecules, and the bromine molecules formed inside of the layer would diffuse to the surface, causing the strong signal.

Conversely, as silver atoms do not diffuse and carbon is contained only in the gelatin, the ratio of silver to carbon would be an indicator of the ratio of silver halide to gelatin. The weight ratio of silver to carbon is 0.47 in Em1 and 1.8 in Em2, a difference of 3.8 times. This suggests that the ratio of silver halide in Em2 is extremely high, as described above.

Characteristic curves obtained by light sensitometry are shown in Fig. 3. The sensitivity of Em1 is 0.40, which is approximately 2.7 times higher than that of Em2, which is 0.15. The fog values are 0.04 in Em1 and 0.02 in Em2. Although both are very small, that of Em2 is slightly smaller. The gamma values are 3.4 for Em1 and 5.1 for Em2. Em2 shows a sharp increase in the characteristic curve and has higher contrast. Therefore, the characteristic curves of Em1 and 2 in the high-exposure region almost overlap, suggesting that both emulsions show similar OD values for such exposure region.

The increase in OD with β-ray irradiation time is shown in Fig. 4. Because the variation of these values in Em2 is larger than that of Em1, the spread of the plotting points is also wider. However, the OD increasing curves for both emulsions are similar ones and indicate that the emulsions show nearly the same result of OD, or have the same sensitivity to β-ray irradiation.

TEM micrographs of developed silver particles are shown in Fig. 5. The top row shows the pictures with low magnification and the

Table 1 Composition analysis of the emulsion layer by EDX

Em1

	1st meas.		2nd meas.		Ave.	
	mass%	atom%	mass%	atom%	mass%	atom%
Ag	21.4	4.6	18.2	3.7	19.8	4.2
Br	27.7	8.0	29.7	8.1	28.7	8.1
C	36.0	69.3	39.1	70.7	37.1	70.0
O	12.3	17.7	13.0	17.6	12.7	17.7

Em2

	1st meas.		2nd meas.		Ave.	
	mass%	atom%	mass%	atom%	mass%	atom%
Ag	34.2	11.7	29.0	10.6	31.6	11.2
Br	42.6	19.7	43.2	21.4	42.9	20.4
C	19.2	59.2	17.3	56.7	18.3	58.0
O	4.1	9.4	3.9	9.5	4.0	9.5

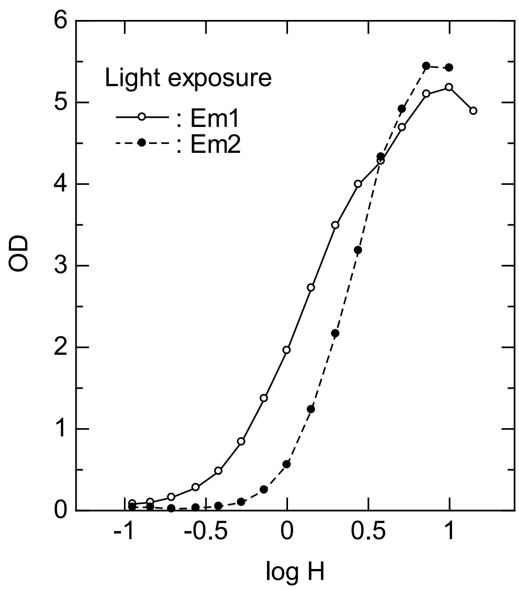

Fig. 3 Photographic characteristic curves for Em1 and 2 exposed to high-intensity light for 10^{-5} s.

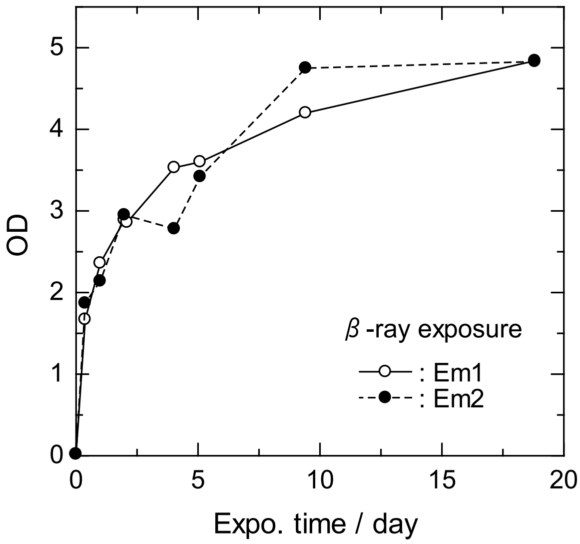

Fig. 4 OD increasing rate for Em1 and 2 during exposure with β-rays emitted from RI of ^{14}C.

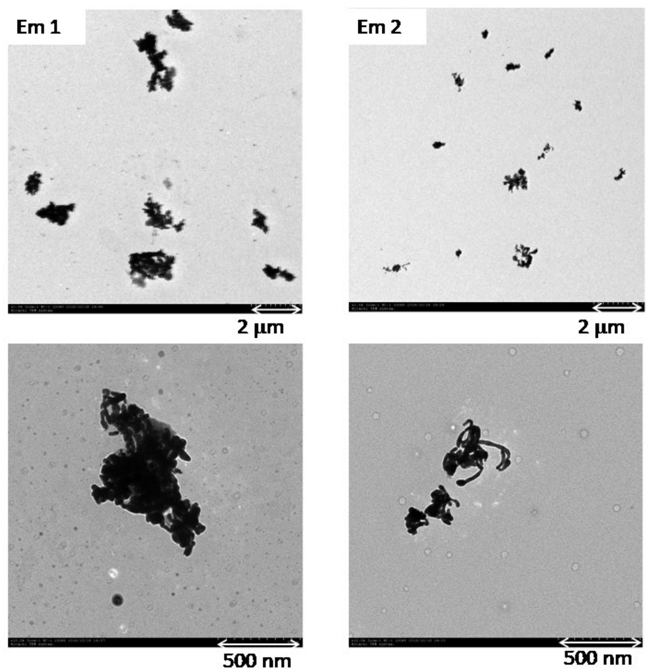

Fig. 5 Transmission electron micrographs of developed silver particles extracted from the high-exposure area of the samples in Fig. 3. Left column: Em1, right column: Em2. Top row: low magnification, bottom row: high magnification of the same area.

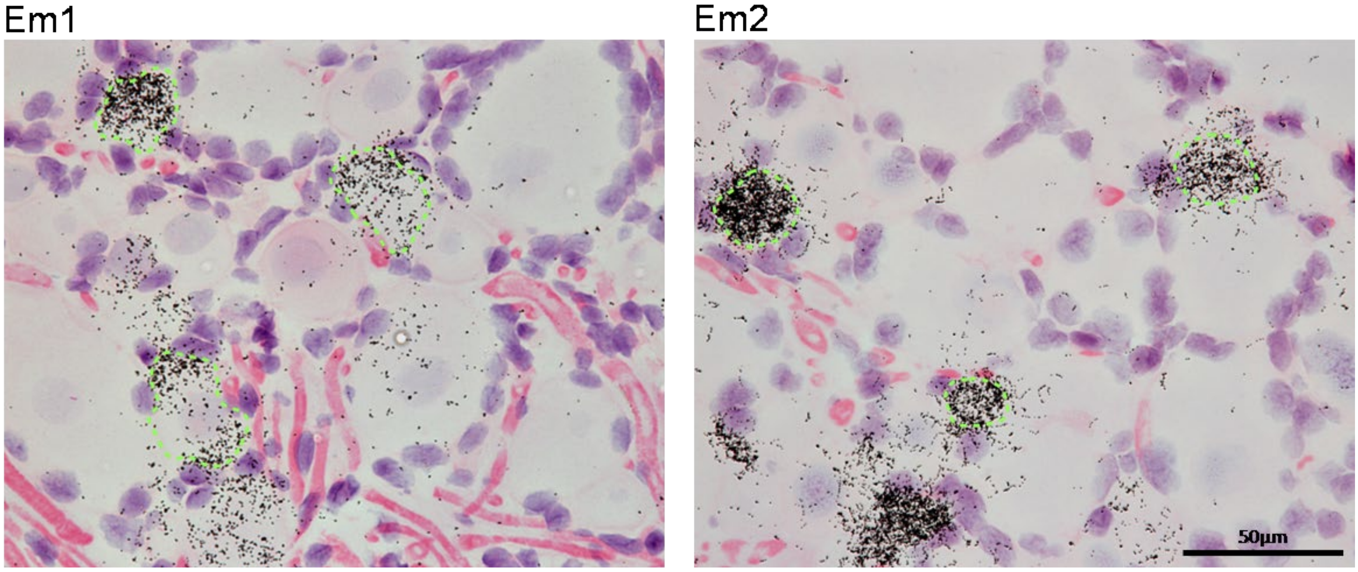

Fig. 6 Autoradiographs by β-rays emitted from RI of ^{35}S observed with an optical microscope for Em1 and 2. Both emulsions were coated on the sample containing RI, and the samples covered with the emulsion layer were developed after storage for 4-8 weeks. Green circles with dashed line indicate the approximate locations of cell membrane which are labeled neurons.

bottom row shows those of the same area with high magnification. Corresponding to the difference in size of the original silver halide grains, that of the developed silver particles for Em1 is also larger than that of Em2 and has a wide size distribution. Both particles have the appearance of a woolen ball with silver filaments, but the ball of Em1 is composed of many relatively thick filaments, while that of Em2 consists of thin filaments.

We conducted *in situ* hybridization histochemistry to compare the optical images between Em1 and 2 in same hybridization probe. Experimental procedure of *in situ* hybridization histochemistry is described previously[13]. Representative images of the autoradiography with labeled compounds of ^{35}S are shown in Fig. 6. Clear distribution images of RI are obtained for both emulsions. The distribution density of the number of developed silver particles in Em2 is greater than that in Em1, which may be due to the higher weight ratio of silver halide in Em2 and the greater number of silver-halide grains contained in Em2 because of its small grain size. Positive cells containing RI are surrounded with green circles in Fig. 6, and the grains of Em2 seems to be scattered around the cells compared with Em1. Although these results indicated some slight differences of optical images between Em1 and 2, Em2 has good performance for autoradiography like Em1.

4. Discussion

The grain shape was primarily hexagonal flat in Em1, and a small amount of rod-shaped and spherical particles were also found, while almost all grains in Em2 were octahedra whose edges and corners were rounded to make them sphere-like. Em1 had a wide size distribution and a wide variety of shapes, while Em2 was composed of nearly monodispersed grains with the same size and same shape. Although the average thickness of the hexagonal grains in Em1 is unknown, it seems that most of the grains in Em1 have larger volume compared with the grains in Em2.

It has been reported that the sensitivity at light exposure is proportional to the volume of silver halide grains [14]. Em1, which has grains of larger volume, has higher sensitivity in light, as determined by the rising point of the characteristic curves. Conversely, emulsions with wide grain-size distribution generally have low contrast, as seen in Em1. Because Em2, with monodispersed grains, has higher contrast, the high-exposure parts of the characteristic curves for Em1 and 2 overlap.

In the case of β-ray irradiation, the amount of energy that a silver halide grain receives will be proportional to the path of one β particle. This causes the sensitivity to be proportional not to the grain volume, but to the diameter. Compared with the light sensitivity, the sensitivity difference for β-ray will be reduced. In addition, because the β particles with an average energy of 167 keV used here have a relatively high energy loss, large numbers of electron and hole pairs are generated, and this is equivalent to the high-exposure region in the characteristic curve. Therefore, the result in Fig. 4 for the β-ray exposure showed almost the same sensitivity for Em1 and 2.

Clear images of autoradiography comparable to Em1 are obtained with Em2. This and the photographic properties mentioned above suggest that Em2 may be useful as an emulsion for autoradiography like Em1.

We have evaluated the properties for autoradiography with both emulsions and obtained fruitful results. However, it is necessary to consider other issues, including the ease of handling, for use in autoradiography.

When we applied emulsion Em2 to a glass base, it showed insufficient wettability to the base and some difficulty to spread. The emulsion layer was sometimes repelled along the peripheral area of the base, leading to some non-uniformity of the layer. This would be one reason for the wide spread of the plotting points in Fig. 4. Em2 was designed to make the ratio of silver halide to gelatin high in order to yield high efficiency for track detection, as mentioned above. An emulsion with less gelatin ratio will cause some randomness in the layer because the silver halide grains themselves are hydrophobic and easy to coagulate. For autoradiography, it will be better to lower the ratio of silver halide by diluting the emulsion with an aqueous solution of gelatin.

In addition, application of the emulsion directly on the sample is expected in the case of autoradiography, and there is a possibility that some samples will repel the emulsion. We did not use additives such as surfactants with the emulsion in this experiment. It is also necessary to study the improvement of the coating property by adding surfactants that do not have any photographic effects.

Conclusion

We investigated the nuclear emulsion produced at Nagoya University by comparing its photographic and autoradiographic properties with an emulsion for autoradiography that is currently commercially available. The obtained autoradiography images indicated the distribution of RI clearly. This emulsion can be used for autoradiography even if the supply of commercial emulsions is discontinued. However, certain details are yet to be considered regarding the coating properties, such as additional gelatin to reduce the ratio of silver halide to gelatin or the addition of surfactants.

References

1) V. Mizuhira, "Isotope Handbook", 3rd ed., by Japan Isotope Association, Maruzen, Tokyo, 1984, Chap.15, Sec.11, (in Japanese).
2) N. Naganawa, T. Fukuda, N. Kitagawa, M. Komatsu, K. Morishima, T. Naka, T. Nakano, A. Nishio, H. Rokujo, O. Sato, Radiation Chemistry, **107**, 35 (2019)(in Japanese).
3) A. Nishio, K. Morishima, K. Kuwabara, T. Yoshida, T. Funakubo, N. Kitagawa, M. Kuno, Y. Manabe, M. Nakamura, Nuclear Instruments and Methods in Phys. Research A, **966**, 163850 (2020).
4) K. Kuwabara, S. Nishiyama, J. Soc. Photogr. Imaging Jpn., **67**, 521 (2004)(in Japanese).
5) T. Toshito, J. Soc. Photogr. Imaging Jpn., **67**, 538 (2004)(in Japanese).
6) K. Morishima, J. Soc. Photogr. Imaging Jpn., **79**, 48 (2016)(in Japanese).
7) K. Morishima, M. Kuno, A. Nishio, N. Kitagawa, Y. Manabe, M. Moto, F. Takasaki, H. Fujii, K. Satoh, H. Kodama, K. Hayashi, S. Odaka, S. Procureur, D. Attie, S. Bouteille, D. Calvet, C. Filosa, P. Magnier, I. Mandjavidze, M. Riallot, B. Marini, P. Gable, Y. Date, M. Sugiura, Y. Elshayeb, E. Tamer, M. Ezzy, E. Guerriero, V. Steiger, N. Serikoff, J. Mouret, B. Charles, H. Helal, M. Tayoubi, Nature, **552**, 386 (2017).
8) S. Takahashi, S. Aoki, GRAINE collaboration, J. Soc. Photogr. Imaging Jpn., **78**, 228 (2015)(in Japanese).
9) O. Sato, M. Komatsu, J. Soc. Photogr. Imaging Jpn., **78**, 212 (2015)(in Japanese).
10) T. Fukuda, S. Aoki, S. Cao, N. Chikuma, Y. Fukuzawa, M. Gonin, T. Hayashino, Y. Hayato, A. Hiramoto, F. Hosomi, K. Ishiguro, S. Iori, T. Inoh, H. Kawahara, H. Kim, N. Kitagawa, T. Koga, R. Komatani, M. Komatsu, A. Matsushita, S. Mikado, A. Minamino, H. Mizusawa, K. Morishima, T. Matsuo, T. Matsumoto, Y. Morimoto, M. Morishita, K. Nakamura, M. Nakamura, Y. Nakamura, N. Naganawa, T. Nakano, T. Nakaya,Y. Nakatsuka, A. Nishio, S. Ogawa, H. Oshima, B. Quilain, H. Rokujo, O. Sato, Y. Seiya, H. Shibuya, T. Shiraishi, Y. Suzuki, S. Tada, S. Takahashi, K. Yamada, M. Yoshimoto, M. Yokoyama, Prog.Theor.Exp. Phys. **2017**, 063C02 (2017).
11) N. Naganawa, K. Ozeki, K. Kuwabara, K. Morishima, H. Rokujo, H. Kawara, A. Nishio, Y. Kato, H. Machii, J. Soc. Photogr. Imaging Jpn., **77**, 117 (2014)(in Japanese).
12) K. Kuge, T. Adachi, A. Umemoto, T. Naka, S. Kodaira, J. Soc. Photogr. Imaging Jpn., **82**, 297 (2019)(in Japanese).
13) M. Okubo, H. Yamanaka, K. Kobayashi, Y. Dai, H. Kanda, H. Yagi, K. Noguchi, PLOS one, April, 12 (2016).
14) T. Tani, "Photographic Sensitivity", Oxford University Press, New York, 1995, p89.